

RSC Advances



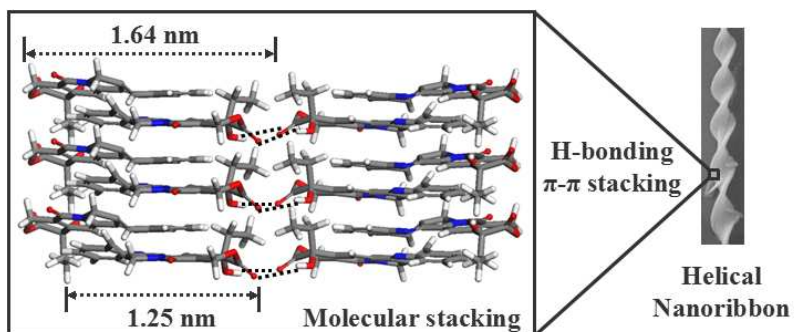
This is an *Accepted Manuscript*, which has been through the Royal Society of Chemistry peer review process and has been accepted for publication.

Accepted Manuscripts are published online shortly after acceptance, before technical editing, formatting and proof reading. Using this free service, authors can make their results available to the community, in citable form, before we publish the edited article. This *Accepted Manuscript* will be replaced by the edited, formatted and paginated article as soon as this is available.

You can find more information about *Accepted Manuscripts* in the [Information for Authors](#).

Please note that technical editing may introduce minor changes to the text and/or graphics, which may alter content. The journal's standard [Terms & Conditions](#) and the [Ethical guidelines](#) still apply. In no event shall the Royal Society of Chemistry be held responsible for any errors or omissions in this *Accepted Manuscript* or any consequences arising from the use of any information it contains.

Graphical abstract



Cite this: DOI: 10.1039/c0xx00000x

www.rsc.org/xxxxxx

ARTICLE TYPE

Reversible pH-responsive helical nanoribbons formed by camptothecin

Mingfang Ma^a, Pengyao Xing^a, Shengguang Xu^b, Shangyang Li^a, Xiaoxiao Chu^a and Aiyou Hao^{a*}

Received (in XXX, XXX) Xth XXXXXXXXXX 20XX, Accepted Xth XXXXXXXXXX 20XX

DOI: 10.1039/b000000x

The natural antitumor drug camptothecin was found to self-assemble into helical nanoribbons in aqueous solution. The helical nanoribbons showed good reversible pH-responsiveness. The formation and disappearance of the helical nanoribbons can be tuned reversibly through changing the pH value of the solution.

The self-assembly of the low-molecular-weight molecule into various hierarchical structures has attracted extensive attention in the past decade.¹⁻⁹ Construction of supramolecular self-assembly with desired structures and properties endows the low-molecular-weight molecules with significant function in the development of soft materials. Low-molecular-weight natural products derivatives are often used to fabricate hierarchical structures. Amino acid¹⁰, peptide¹¹ and sugar^{12, 13} derivatives can all be the building blocks of self-assembly. However, the sophisticated ordered aggregates from natural products have rarely been reported, especially for chiral structures, attributing to their complex structures. On the contrary, the chiral structures are mostly constructed by carefully designed molecules.

Chirality is one of the most significant phenomena found in nature. It is essential to complicated biological activities in living system, for instance, DNA with helical double chain structures plays an important role in heredity. Chiral nanostructures, including nanotwists¹⁴, nanoribbons¹⁵ and rolled-up nanotubes¹⁶, have received great interest because of their unique structures and potential applications in the field of separation, catalysis and supramolecular electronics.¹⁷⁻¹⁹ The chirality of those nanostructures can be derived from non covalent interactions^{20, 21}, such as van der Waals, π - π stacking, H-bonding, coordination and so on. Chiral nanostructures are often constructed by chiral molecules whereby the chirality of chiral molecules determines the chirality of chiral nanostructures. Compared with the molecular chirality, the chirality of chiral nanostructures could be easily regulated by external stimuli, such as environmental temperature, pH, photo irradiation, solvents and so on²²⁻²⁶, allowing chiral nanostructures with some new functions than the sole chiral molecules. Although, many researches based on chiral nanostructures from low-molecular-weight molecules have been reported, as far as we know the chiral nanostructures fabricated directly from natural camptothecin (CPT) have never been reported in anywhere.

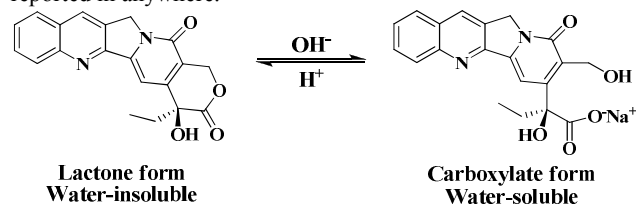


Fig. 1 Camptothecin structure and pH-dependent equilibrium between water-insoluble lactone form and water soluble carboxylate form.

CPT, which was first isolated from Chinese tree *Camptotheca acuminata* in 1960s, has shown a wide spectrum of anticancer activity against various kinds of human cancers.^{27, 28} The terminal ring of CPT can be converted reversibly between the lactone form in acidic environment and the carboxylate form in basic environment, just as illustrated in Fig. 1.^{29, 30} The chiral lactone form of CPT is water insoluble, while the carboxylate form of CPT is water soluble. Meanwhile, CPT has a well-understood rigid and planar geometric π -conjugated structure, making it a good candidate for the construction of advanced supramolecular nanomaterials. Those unique properties may allow us to design pH-responsive functional self-assembly based on CPT. The chiral nanostructures may be fabricated by CPT, since CPT is a chiral molecule. Moreover, the obtained chiral nanostructures may have pH-responsiveness, attributing to the pH-responsive transformation between different forms of CPT.

Herein, we report an interesting chiral nanostructure self-assembled from natural CPT. The lactone form CPT molecules self-assembled into helical nanoribbons, whereas the carboxylate form CPT molecules dispersed uniformly in aqueous solution and hence could not form any aggregate. Moreover, the transformation between helical nanoribbon and non-aggregate can be tuned reversibly by changing the pH value of sample aqueous solution. To best our knowledge, the helical nanoribbon constructed by natural antitumor drug CPT has never been reported previously.

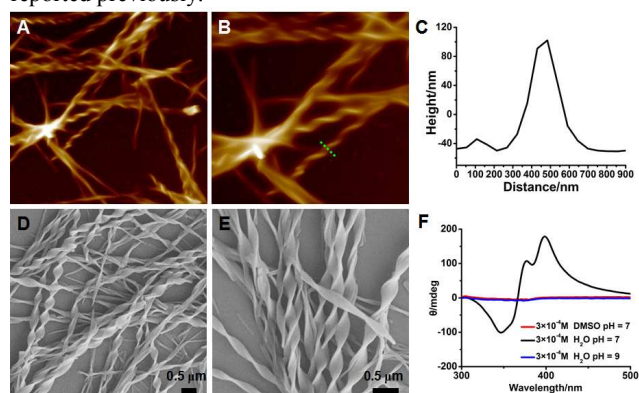


Fig. 2 (A) AFM image of CPT samples (3×10^{-4} mol/L) at room temperature; (B) the amplified image of (A); (C) the nanoribbon diameter curve which is consistent with the marked green line in (B); (D) SEM image of CPT samples (3×10^{-4} mol/L) at room temperature; (E) the amplified SEM image of CPT samples; (F) the circular dichroism spectra comparison of CPT in different solvents and pH values.

The molecular structures of CPT are shown in Fig. 1. Although the lactone form of CPT is water-insoluble, the carboxylate form of CPT is water-soluble. The lactone form and carboxylate form of CPT can be tuned reversible by changing the pH value. The 10^{-2} mol/L mother dimethylsulfoxide (DMSO) solution was prepared by dissolving certain molar quantities of powder CPT in DMSO directly. Then the self-assembly of lactone form CPT was obtained by injecting CPT mother DMSO solution into distilled water, making the concentration of CPT to 3×10^{-4} mol/L. The colloidal solution was formed after the mixing process (Fig. S1A). To investigate what is in the colloidal solution, atomic force microscopy (AFM) and scanning electron microscopy (SEM) were used in our study. As shown in Fig. 2A-C, the helical nanoribbons with the diameter of 100-400 nm and the length of 4-24 μm were found under AFM. Meanwhile, the morphologies and sizes of CPT helical nanoribbons were further confirmed by SEM, which is shown in Fig. 2D and Fig. 2E. Hence, the lactone form CPT can self-assemble into helical nanoribbons in the poor solvent. Circular dichroism (CD) spectra comparison can further verify that helical structures exist in the CPT aqueous solution since obvious Cotton effects can be observed in Fig. 2F.³¹⁻³³ On the contrary, there is no Cotton effects can be found in DMSO solution of CPT, indicating that single molecular state CPT in DMSO can not self-assemble into well-defined aggregates. In addition, based on AFM and SEM results, we can find that the nanoribbons exhibit right-handed helicity (P type), indicating that the nanoribbons are kinetically controlled³⁴⁻³⁶. It is reasonable since the nanoribbons can be formed immediately after injecting CPT DMSO solution into distilled water.

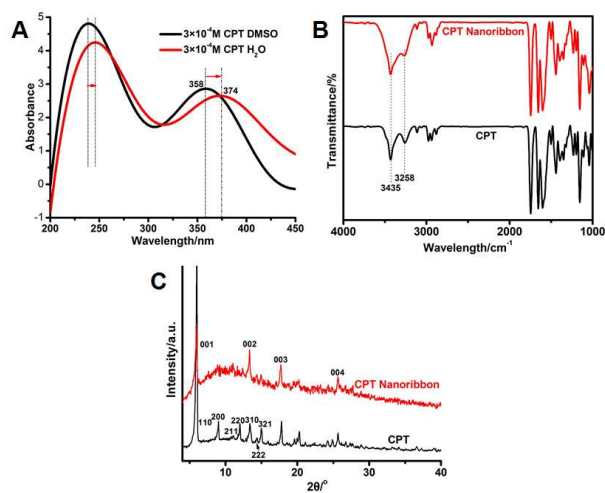


Fig. 3 (A) UV-vis spectra comparison of CPT in DMSO and H₂O; (B) FT-IR spectra comparison of CPT and CPT nanoribbons; (C) XRD pattern comparison of CPT and CPT nanoribbons.

In order to study the helical nanoribbons formation mechanism, the ultraviolet-visible (UV-vis) spectrum, Fourier transform infrared (FT-IR) spectroscopy and X-ray diffraction (XRD) were employed. Fig. 3A displays the UV-vis spectra comparison of CPT in different solvent at pH = 7. CPT should be in lactone form in neutral H₂O and DMSO. CPT molecules in DMSO should be in a single molecule state for their good solubility in DMSO. However, CPT molecules in H₂O should be another state for their low solubility in H₂O. The main absorption peak of CPT in H₂O exhibits an obvious red shift than that in DMSO from 358 nm to 374 nm, indicating the formation of J-type π - π stacking molecular model.³⁷ Hence, π - π stacking may be one of the driving forces for constructing the nanoribbons. Meanwhile, the UV-vis

absorbance intensity of CPT in H₂O is decreased obviously than that in DMSO. The decrease is consistent with the nanoribbons assembly, reducing the number of CPT molecules in H₂O attributing to its low solubility, which can further verify the formation of aggregates in the aqueous solution. FT-IR, which can provide the information about H-bonds, was used to investigate the driving force of helical nanoribbons formation.³⁸ As shown in Fig. 3B, the characteristic absorption peaks ($\nu_{\text{OH}} = 3435 \text{ cm}^{-1}$ and ν_{OH} of intramolecular hydrogen bond = 3258 cm^{-1}) of CPT can all be found in the curves of CPT and CPT helical nanoribbons. However, the ν_{OH} of intramolecular hydrogen bond = 3258 cm^{-1} in CPT becomes smaller in CPT nanoribbons, moreover, the peak of $\nu_{\text{OH}} = 3435 \text{ cm}^{-1}$ in CPT nanoribbons becomes broad, indicating the formation of H-bonds between different CPT molecules. So H-bonding may be one driving force for helical nanoribbon formation too. Meanwhile, the triplet around 2940 cm^{-1} in CPT nanoribbon, which belongs to $\nu_{\text{C-H}}$ of alkyl, also changed obviously than that in natural CPT, meaning that there should be different molecule stacking style between CPT nanoribbon and natural CPT. To investigate more detailed microstructure information of CPT helical nanoribbons, XRD was used in our study.³⁹ From Fig. 3C, we can find that the XRD pattern of CPT nanoribbons is different from that of CPT. Many diffraction peaks appear in CPT pattern with $\sin^2\theta$ ratio of 1:2:3:4:5:6:7, which is consistent with a body centered cubic stacking pattern, indicating that CPT is a typical crystal.⁴⁰ However, four diffraction peaks appear in CPT nanoribbons with d values of 1.64 nm, 0.81 nm, 0.55 nm and 0.40 nm based on Bragg equation, and their ratio is 1: 0.5: 0.33: 0.25, indicating a lamellar structure in CPT nanoribbons. The layer spacing was calculated to be 1.64 nm, is in agree with the length of two CPT molecules (calculated about 1.25 nm per CPT molecule from Material Studio 5.5) with large overlapped stacking area.

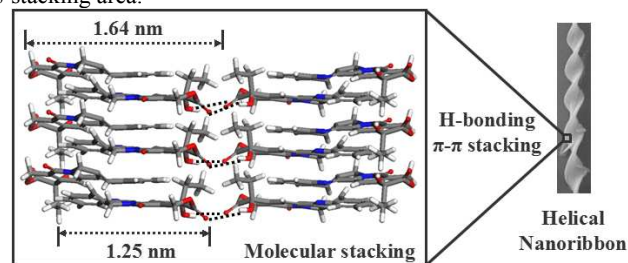


Fig. 4 Schematic illustration of molecules arrangements in CPT helical nanoribbons, dashed lines represent intermolecular H-bonds.

On basis of the above analysis, π - π stacking and H-bonding between different CPT molecules may be the main driving forces to induce the formation of CPT helical nanoribbons. The plausible mechanism of molecular stacking in CPT helical nanoribbons is proposed in Fig. 4. The lactone form CPT molecules stacked in a body centered cubic stacking pattern in natural CPT crystal. The lactone form CPT molecules dispersed uniformly in DMSO and were in single molecule states when the natural CPT crystal was dissolved in DMSO. Then the single lactone form CPT molecules self-assembled into nanoribbons attributing to intermolecular H-bonds and π - π stacking when CPT DMSO solution was diluted by deionized water. Different lactone form CPT molecules can closely pack together through π - π stacking, and different array molecules can link together by H-bonds. The helical nanoribbons were formed in this process, since π - π stacking model between two CPT molecules is J-type with asymmetric packing.

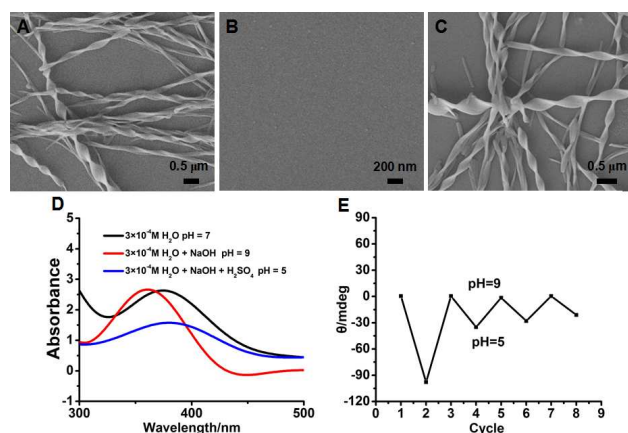


Fig. 5 (A) SEM image of CPT samples (3×10^{-4} mol/L) at room temperature (pH = 7); (B) SEM image of CPT samples in (A) treated with sodium hydroxide (pH = 9); (C) SEM image of CPT samples in (B) treated with sulfuric acid (pH = 5); (D) UV-vis spectra comparison of CPT aqueous solution in different pH values; (E) CD spectra intensity of CPT samples during several pH-responsive cycles.

It is interesting that the CPT helical nanoribbons exhibit good reversible pH-responsiveness. As shown in Fig. 5A-C, the SEM morphologies of the helical nanoribbons disappeared after a certain amount of sodium hydroxide was added into the CPT aqueous solution (pH = 9). More interesting is that the helical nanoribbons reappeared after a certain amount of sulfuric acid was further added into the CPT alkaline solution (pH = 5). The transformation even can be found by the naked eyes. Fig. S1 shows that the colloidal solution of lactone form CPT turned into clear solution after sodium hydroxide was added into the CPT aqueous solution. The clear solution turned into the colloidal solution again after sulfuric acid was added into the CPT alkaline solution. This transformation can be further verified by UV-vis spectrum (Fig. 5D). The main absorption peak of lactone form CPT in H₂O is around 374 nm. After sodium hydroxide was added into the CPT aqueous solution, the lactone form CPT turned into the carboxylate form CPT, the main absorption peak of CPT alkaline solution shifted to 360 nm, indicating the existence of single molecular carboxylate form CPT. After sulfuric acid was added into the CPT alkaline solution, the carboxylate form CPT turned into the lactone form CPT, the main absorption peak of CPT acid solution was back to around 374 nm again, indicating the formation of lactone form CPT aggregates. CD spectra comparison confirms that this transformation can repeat at least 4 times. As shown in Fig. 5E and Fig S2, there is almost no CD signal in the CPT alkaline solution. However, strong Cotton effects can be found in CPT acid solution. The appearance and disappearance of Cotton effects can be tuned several times through changing the pH value of CPT aqueous solution.

Conclusions

In summary, we have successfully constructed a novel helical nanoribbon based on natural antitumor drug CPT. Due to the unique structure of CPT, the formation and disappear of helical nanoribbons can be tuned reversibly by changing the pH value of the solution. These results can not only help us to further understand the supramolecular chiral self-assembly, but also pave the avenue to construct novel functional helical soft materials from natural drugs.

Notes and references

- ^aSchool of Chemistry and Chemical Engineering and Key Laboratory of Colloid and Interface Chemistry of Ministry of Education, Shandong University, Jinan 250100, China. E-mail: haoay@sdu.edu.cn.; Fax: +86-531-88564464; Tel.: +86-531-88363306;
- ^bCollege of Chemistry and Materials Science, Ludong University, Yantai 264025, P. R. China.
- 1 C. Z. Wang, Q. Gao and J. B. Huang, *Langmuir*, 2003, **19**, 3757-3761.
 - 2 Y. Zhao, J. Zhao, Y. Yan, Z. C. Li and J. B. Huang, *Soft Matter*, 2010, **6**, 3282-3288.
 - 3 Y. Y. Lin, Y. Qiao, P. F. Tang, Z. B. Li and J. B. Huang, *Soft Matter*, 2011, **7**, 2762-2769.
 - 4 M. F. Wang, A. R. Mohebbi, Y. M. Sun and F. Wudl, *Angew. Chem. Int. Ed.*, 2012, **51**, 6920-6924.
 - 5 K. Wang, C. Y. Wang, Y. Wang, H. Li, C. Y. Bao, J. Y. Liu, X. A. Zhang and Y. W. Yang, *Chem. Commun.*, 2013, **49**, 10528-10530.
 - 6 P. C. Zhang, A. G. Cheetham, Y. A. Li and H. G. Cui, *ACS Nano*, 2013, **7**, 5965-5977.
 - 7 P. Y. Xing, X. X. Chu, G. Y. Du, M. Z. Li, J. Su, A. Y. Hao, Y. H. Hou, S. Y. Li, M. F. Ma, L. Wu and Q. B. Yu, *RSC Adv.*, 2013, **3**, 15237-15244.
 - 8 A. G. Cheetham, Y. C. Ou, P. C. Zhang and H. G. Cui, *Chem. Commun.*, 2014, **50**, 6039-6042.
 - 9 H. G. Cui, A. G. Cheetham, E. T. Pashuck and S. I. Stupp, *J. Am. Chem. Soc.*, 2014, DOI: 10.1021/ja507051w.
 - 10 S. Ahmed, J. H. Mondal, N. Behera and D. Das, *Langmuir*, 2013, **29**, 14274-14283.
 - 11 Y. T. Fu, B. Z. Li, Z. B. Huang, Y. Li and Y. G. Yang, *Langmuir*, 2013, **29**, 6013-6017.
 - 12 Y. Y. Lin, Y. Qiao, C. Gao, P. F. Tang, Y. Liu, Z. B. Li, Y. Yan and J. B. Huang, *Chem. Mater.*, 2010, **22**, 6711-6717.
 - 13 T. Sun, Q. Guo, C. Zhang, J. C. Hao, P. Y. Xing, J. Su, S. Y. Li, A. Y. Hao and G. C. Liu, *Langmuir*, 2012, **28**, 8625-8636.
 - 14 H. Cao, X. F. Zhu and M. H. Liu, *Angew. Chem. Int. Ed.*, 2013, **52**, 4122-4126.
 - 15 R. Oda, F. Artzner, M. Laguerre and I. Huc, *J. Am. Chem. Soc.*, 2008, **130**, 14705-14712.
 - 16 S. Shin, S. Lim, Y. Kim, T. Kim, T. L. Choi and M. Lee, *J. Am. Chem. Soc.*, 2008, **130**, 2156-2159.
 - 17 E. Yashima, K. Maeda, H. Iida, Y. Furusho and K. Nagai, *Chem. Rev.*, 2009, **109**, 6102-6211.
 - 18 Y. Yang, Y. J. Zhang and Z. X. Wei, *Adv. Mater.*, 2013, **25**, 6039-6049.
 - 19 J. V. Herrikhuyzen, A. Syamakumari, A. Schenning and E. W. Meijer, *J. Am. Chem. Soc.*, 2004, **126**, 10021-10027.
 - 20 P. Y. Xing, X. X. Chu, M. F. Ma, S. Y. Li and A. Y. Hao, *Phys. Chem. Chem. Phys.*, 2014, **16**, 8346-8359.
 - 21 Y. Qiao, Y. J. Wang, Z. Y. Yang, Y. Y. Lin and J. B. Huang, *Chem. Mater.*, 2011, **23**, 1182-1187.
 - 22 Y. Q. Liu, T. Y. Wang, Z. B. Li and M. H. Liu, *Chem. Commun.*, 2013, **49**, 4767-4769.
 - 23 Q. X. Jin, L. Zhang and M. H. Liu, *Chem. Eur. J.*, 2013, **19**, 9234-9241.
 - 24 C. X. Liu, Q. X. Jin, K. Lv, L. Zhang and M. H. Liu, *J. Name.*, 2012, **00**, 1-3.
 - 25 L. Zhang, L. Qin, X. F. Wang, H. Cao and M. H. Liu, *Adv. Mater.*, 2014, DOI: 10.1002/adma.201305422.
 - 26 Y. Qiao, Y. Y. Lin, Z. Y. Yang, H. F. Chen, S. F. Zhang, Y. Yan and J. B. Huang, *J. Phys. Chem. B*, 2010, **114**, 11725-11730.
 - 27 R. Kunii, H. Onishi and Y. Machida, *Eur. J. Pharm. Biopharm.*, 2007, **67**, 9-17.

- 28 K. M. Tyner, S. R. Schiffman and E. P. Giannelis, *J. Control. Release*, 2004, **95**, 501-514.
- 29 Y. Çirpanli, E. Bilensoy, A. L. Dogan and S. Çalis, *Eur. J. Pharm. Biopharm.*, 2009, **73**, 82-89.
- 5 30 J. J. Chen, K. T. Khin and M. E. Davis, *Mol. Pharm.*, 2004, **1**, 183-193.
- 31 L. Xu, L. Feng, R. H. Dong, J. C. Hao and S. L. Dong, *Biomacromolecules*, 2013, **14**, 2781-2789.
- 32 L. L. Lock, M. LaComb, K. Schwarz, A. G. Cheetham, Y. A. Li, P. C. Zhang and H. G. Cui, *Faraday Discuss.*, 2013, **166**, 285-301.
- 10 33 A. G. Cheetham, P. C. Zhang, Y. A. Li, L. L. Lock and H. G. Cui, *J. Am. Chem. Soc.*, 2013, **135**, 2907-2910.
- 34 P. Y. Xing, X. X. Chu, S. Y. Li, M. F. Ma and A. Y. Hao, *Chem. Phys. Chem.*, 2014, **15**, 1-10.
- 15 35 C. C. Lee, C. Grenier, E. W. Meijer and A. P. Schenning, *Chem. Soc. Rev.*, 2009, **38**, 671-683.
- 36 P. A. Korevaar, S. J. George, A. J. Markvoort, M. M. Smulders, P. A. Hilbers, A. P. Schenning, T. F. Greef and E. W. Meijer, *Nature*, 2012, **481**, 492-497.
- 20 37 Y. Qiao, Y. Y. Lin, S. Liu, S. F. Zhang, H. F. Chen, Y. J. Wang, Y. Yan, X. F. Guo and J. B. Huang, *Chem. Commun.*, 2013, **49**, 704-706.
- 38 P. Y. Xing, X. X. Chu, S. Y. Li, F. F. Xin, M. F. Ma and A. Y. Hao, *New J. Chem.*, 2013, **37**, 3949-3955.
- 25 39 C. Wang, S. C. Yin, S. L. Chen, H. P. Xu, Z. Q. Wang and X. Zhang, *Angew. Chem.*, 2008, **120**, 9189-9192.
- 40 X. H. Zhao, Y. G. Zu, Q. Y. Li, M. X. Wang, B. S. Zu, X. N. Zhang, R. Jiang and C. L. Zu, *J. of Supercritical Fluids*, 2010, **51**, 412-419.
- 30